Acta Cryst. (1997). C**53**, 1526–1529

Sb_2MoO_6, a Re-examination

Alicia Castro,† Renée Enjalbert and Jean Galy

Centre d'Elaboration de Matériaux et d'Etudes Structurales, CNRS, 29 rue Jeanne Marvig, BP 4347, 31055 Toulouse CEDEX, France. E-mail: enjalber@cemes.fr

(Received 2 December 1996; accepted 23 April 1997)

Abstract

Single crystals of diantimony molybdenum hexaoxide have been grown by solid-state reaction. This oxide crystallizes as a layered structure, as in the case of the previously reported Sb_2WO_6. Mo atoms are located in severely distorted O-atom octahedra while each Sb atom is bonded to five O atoms, three at short distances and two at longer distances, retaining the three-dimensional array.

Comment

Several investigations of the bismuth oxide-based Aurivillius family $(Bi_2O_2)(A_{n-1}B_nO_{3n+1})$ have been devoted to changes in both structural characteristics and properties (A = Na^+, K^+, Ca^{2+}, Sr^{2+}, Pb^{2+}, La^{3+}, Bi^{3+}...; B = Fe^{3+}, Cr^{3+}, Ti^{4+}, Nb^{5+}, Mo^{6+}, W^{6+}...). Recent papers have shown that other lone-pair cations, such as Sn^{II}, Sb^{III} or Te^{IV}, can be partially introduced in the Bi_2O_2 layers (Castro, Millan, Martinez-Lope & Torrance, 1993; Castro, Millan & Enjalbert, 1995; Millan, Ramirez & Castro, 1995), or in the particular $n = 1$ Aurivillius-like phase, where Bi^{III} can be completely replaced by Sb^{III} (Castro, Millan, Enjalbert, Snoeck & Galy, 1994; Ling, Withers, Rae, Schmid & Thompson, 1996; Ramirez, Enjalbert, Rojo & Castro, 1997) to obtain Sb_2WO_6 and $Sb_2(W,V)O_{6-\delta}$ compounds. Indeed, Sb_2WO_6 was first described as an ordered intergrowth between $[Sb_2O_2]_n$ and $[WO_4]_n$ perovskite-type layers and was refined from a twinned crystal in the space group $P1$, with unit-cell parameters a = 5.554 (1), b = 4.941 (2), c = 9.209 (3) Å, α = 90.05 (3), β = 96.98 (2), γ = 90.20 (2)° (Castro, Millan, Enjalbert, Snoeck & Galy, 1994). Subsequently, following electron-microscopy investigations, this structure was further refined as an enlarged $2a \times 2b \times 2c$ F-centred superstructure of the one previously reported, the twinning of crystals being successfully modelled during refinement (Ling, Withers, Rae, Schmid & Thompson, 1996).

In the paper by Ling *et al.* (1996), the authors report the synthesis of a new Sb_2MoO_6 powder phase, giving evidence of its isostructuralism with Sb_2WO_6 and proposing the $F1$ unit cell a = 10.758 (1), b = 9.673 (2), c = 17.57 (1) Å, α = 90.00 (5), β = 96.98 (3), γ = 90.05 (2)°. In fact, other authors (Laarif, Theobald, Vivier & Hewat, 1984) had determined, prior to this proposal, the structure of this oxide by single-crystal X-ray diffraction and powder neutron diffraction methods, resulting, respectively, in the unit-cell parameters a = 7.481 (2), b = 7.504 (2), c = 10.120 (2) Å, α = 70.43 (2), β = 70.91 (2), γ = 83.35 (2)°, and a = 7.4774 (2), b = 7.5017 (2), c = 10.1259 (2) Å, α = 70.374 (1), β = 70.889 (1), γ = 83.246 (1)°.

To ascertain the true structure of Sb_2MoO_6, single crystals were grown by solid-state reaction. From X-ray investigations using the precession method, the superstructure of Sb_2MoO_6 was clearly shown, giving the enlarged cell and a superstructure similar to those of Sb_2WO_6, as demonstrated by transmission electron microscopy experiments. The structure of the title compound has been determined by classic X-ray single-crystal diffraction methods.

The general framework of Sb_2MoO_6 (Fig. 1) maintains the layered arrangement seen for Sb_2WO_6 (Castro *et al.*, 1994; Ling *et al.*, 1996), and is formed by antimony–oxygen double layers alternating with molybdenum–oxygen slabs parallel to the (001) plane, which bind together along the [001] direction through Sb—O bonds. Mo atoms occupy eight independent positions and each bonds to four O atoms at shorter dis-

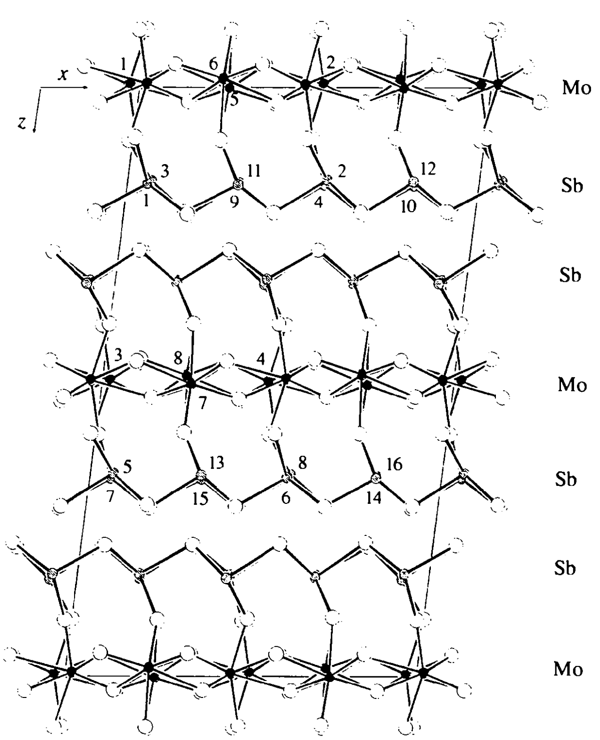

Fig. 1. Projection of the crystal structure of Sb_2MoO_6 onto the (010) plane.

---

† Also affiliated to: Instituto de Ciencia de Materiales de Madrid, CSIC, Cantoblanco, 28049 Madrid, Spain.

tances between 1.739 (8) and 1.935 (7) Å, with an average value ⟨Mo—O⟩ = 1.816 Å, and to two other atoms at longer distances between 2.162 (7) and 2.267 (8) Å (⟨Mo—O⟩ = 2.227 Å). The O atoms thus form strongly distorted octahedra. The Mo atoms are shifted out of their centres as shown in Fig. 2; the displacements range from 0.33 Å for Mo7 to 0.36 Å for Mo4. The MoO_6 octahedra share corners and allow the formation of $[MoO_4]_n$ puckered layers parallel to the (001) plane (Fig. 2).

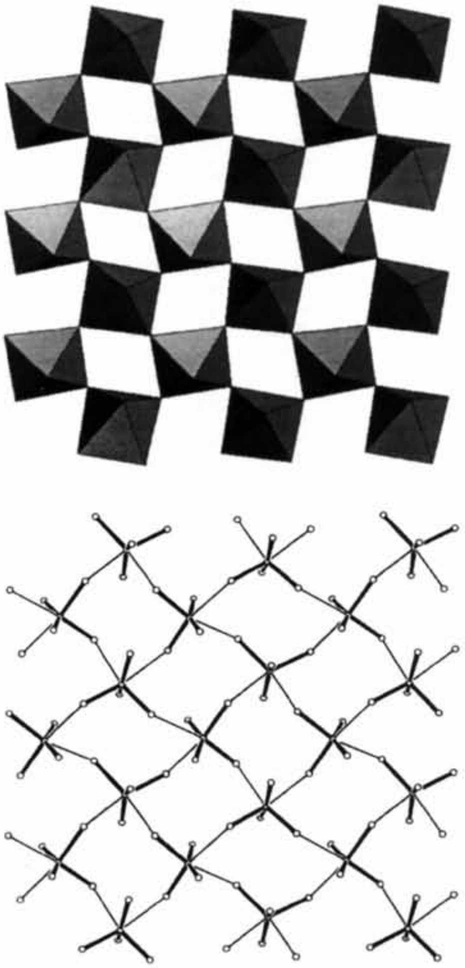

Fig. 2. Projection onto the (001) plane of one $[MoO_4]_n$ layer showing the tilting of the Mo–O octahedra (above) and the Mo—O bonds (dark lines corresponding to short distances) (below).

There exist 16 unequivalent Sb atoms in the unit cell of the Sb_2MoO_6 structure, exhibiting the classic one-sided coordination of cations possessing lone pairs. Each Sb atom is coordinated to three O atoms at short distances, between 1.940 (6) and 2.166 (7) Å (⟨Sb—O⟩ = 2.036 Å) and forms, with two of these O atoms, part of a puckered layer; the third O atom belongs to an apex of an octahedra in the $[MoO_4]_n$ slab. The metal-atom environment is supplemented by two other O atoms at longer distances, between 2.304 (7) and 2.806 (8) Å (⟨Sb—O⟩ = 2.540 Å), joining both $[Sb_2O_2]_n$ layers and the apices of the $[MoO_4]_n$ layer. In all cases, the next shortest Sb—O distance is greater than 3.15 Å. Fig. 3 shows the coordination of some representative Sb atoms together with the possible location of their associated lone pairs, *E*. The coordination of Sb atoms must always be represented as 3+2 where the three short distances are almost regular while the longer distances involve either similar values (*e.g.* Sb2 or Sb12) or different ones (*e.g.* Sb6 or Sb10). The location of the lone pair, *E*, associated with each Sb atom was carried out according to Galy, Meunier, Andersson & Åström (1975); the Sb—*E* distances range from 0.9 to 1.1 Å.

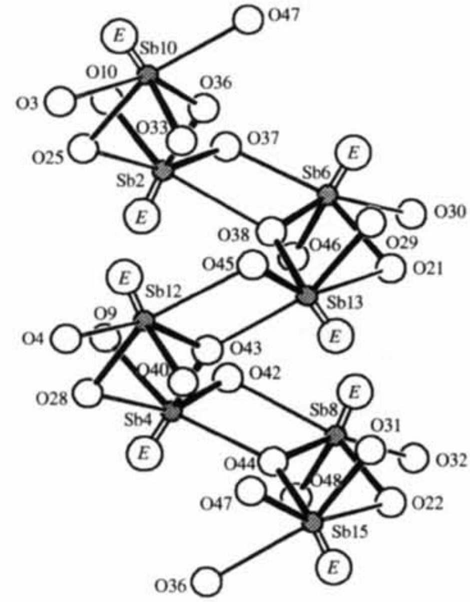

Fig. 3. Coordination polyhedra of representative Sb atoms in Sb_2MoO_6 including lone pairs, *E*.

The thermal study of Sb_2MoO_6 has highlighted an effect at lower temperatures which could be correlated with a rearrangement of the polyhedra in the same way as for Bi_2MoO_6 at low temperatures (van den Elzen & Rieck, 1973) or high temperatures (Buttrey, Vogt, Wildgruber & Robinson, 1994). A study of the low-temperature structure of Sb_2MoO_6 is underway.

Finally, as the structure of Sb_2MoO_6 is highly complex (72 independent atoms corresponding to 16 Sb_2MoO_6 entities) extrapolation of the unit-cell parameters from powder pattern data of a possible non-monophasic sample may account for the wrong values reported by Ling *et al.* (1996), while the parameters proposed by Laarif *et al.* (1984) correspond to a mean structure. Indeed, the matrix [−1 −1 0, −1 1 0, 1 1 −2] transforms their unit-cell parameters to those of the present structure, multiplying the volume by 4.

Experimental

Single crystals of Sb_2MoO_6 were obtained from a mixture of Sb_2O_3 and MoO_3 oxides in the molar ratio 1.5:1, the excess Sb_2O_3 acting as flux. The mixture was ground in an agate mortar and placed in a Pyrex ampoule sealed under vacuum in order to avoid any oxidation of Sb^{III} to Sb^{V}. It was heated at 763 K for 24 h and cooled to room temperature at 5 K h^{-1}.

Crystal data

Sb_2MoO_6
$M_r = 435.44$
Triclinic
$P\overline{1}$
$a = 11.192\,(2)$ Å
$b = 9.9600\,(10)$ Å
$c = 18.282\,(2)$ Å
$\alpha = 90.33\,(3)°$
$\beta = 97.03\,(2)°$
$\gamma = 90.19\,(2)°$
$V = 2022.6\,(5)$ Å^3
$Z = 16$
$D_x = 5.720$ Mg m^{-3}
D_m not measured

Mo $K\alpha$ radiation
$\lambda = 0.71069$ Å
Cell parameters from 25 reflections
$\theta = 9.11–18.23°$
$\mu = 13.001$ mm^{-1}
$T = 293\,(2)$ K
Parallelepiped
$0.252 \times 0.125 \times 0.094$ mm
Red–orange

Data collection

Enraf–Nonius CAD-4 diffractometer
ω–2θ scans
Absorption correction:
  ψ scans (North, Phillips & Mathews, 1968)
  $T_{\min} = 0.21$, $T_{\max} = 0.35$
10 164 measured reflections
6615 independent reflections

2398 reflections with $I > 2\sigma(I)$
$R_{\rm int} = 0.018$
$\theta_{\max} = 26.97°$
$h = -14 \rightarrow 14$
$k = -12 \rightarrow 12$
$l = -23 \rightarrow 23$
6 standard reflections every 200 reflections intensity decay: 0.2%

Refinement

Refinement on F^2
$R[F^2 > 2\sigma(F^2)] = 0.030$
$wR(F^2) = 0.107$
$S = 1.010$
6615 reflections
410 parameters
$w = 1/[\sigma^2(F_o^2) + (0.0509P)^2 + 15.6700P]$ where $P = (F_o^2 + 2F_c^2)/3$
$(\Delta/\sigma)_{\max} = 0.073$

$\Delta\rho_{\max} = 2.61$ e Å^{-3} at 0.35 Å from Sb2
$\Delta\rho_{\min} = -2.85$ e Å^{-3} at 0.78 Å from Sb11
Extinction correction: *SHELXL*96 (Sheldrick, 1996)
Extinction coefficient: 0.0142 (2)
Scattering factors from *International Tables for Crystallography* (Vol. C)

Table 1. *Selected geometric parameters (Å)*

Mo1—O1	1.762 (7)	Sb3—O41	2.568 (6)
Mo1—O2	1.778 (7)	Sb4—O42	1.971 (7)
Mo1—O3	1.832 (7)	Sb4—O43	1.993 (7)
Mo1—O4	1.932 (7)	Sb4—O9$^{\rm iii}$	2.144 (7)
Mo1—O5	2.205 (6)	Sb4—O44	2.330 (7)
Mo1—O6	2.246 (8)	Sb4—O28$^{\rm iii}$	2.690 (7)
Mo2—O7	1.745 (7)	Sb5—O45	1.983 (7)
Mo2—O8	1.775 (7)	Sb5—O16	2.043 (7)
Mo2—O9	1.820 (7)	Sb5—O35$^{\rm vi}$	2.049 (7)
Mo2—O10	1.908 (7)	Sb5—O33$^{\rm vi}$	2.557 (8)
Mo2—O11	2.215 (8)	Sb5—O29	2.615 (8)
Mo2—O12	2.249 (6)	Sb6—O46	1.979 (7)
Mo3—O13	1.751 (7)	Sb6—O38$^{\rm v}$	2.005 (7)
Mo3—O14	1.765 (7)	Sb6—O21	2.097 (7)
Mo3—O15	1.834 (7)	Sb6—O37$^{\rm v}$	2.304 (7)
Mo3—O16	1.930 (7)	Sb6—O30$^{\rm v}$	2.728 (7)
Mo3—O17	2.225 (7)	Sb7—O47	1.978 (7)
Mo3—O18	2.239 (8)	Sb7—O41$^{\rm viii}$	2.039 (6)
Mo4—O19	1.743 (7)	Sb7—O15$^{\rm viii}$	2.154 (7)
Mo4—O20	1.774 (7)	Sb7—O40$^{\rm viii}$	2.337 (7)
Mo4—O21	1.862 (7)	Sb7—O31	2.750 (7)
Mo4—O22	1.935 (7)	Sb8—O48	1.980 (7)
Mo4—O23	2.224 (6)	Sb8—O22$^{\rm vii}$	2.024 (7)
Mo4—O24	2.267 (8)	Sb8—O44$^{\rm vii}$	2.028 (7)
Mo5—O12	1.747 (6)	Sb8—O42$^{\rm vii}$	2.520 (8)
Mo5—O5	1.770 (6)	Sb8—O32$^{\rm vii}$	2.584 (8)
Mo5—O25	1.851 (8)	Sb9—O37	2.025 (7)
Mo5—O26	1.894 (7)	Sb9—O34	2.036 (7)
Mo5—O2$^{\rm i}$	2.173 (7)	Sb9—O26	2.051 (7)
Mo5—O8$^{\rm ii}$	2.233 (7)	Sb9—O48$^{\rm vii}$	2.504 (7)
Mo6—O11	1.741 (8)	Sb9—O10	2.534 (6)
Mo6—O6	1.757 (8)	Sb10—O33$^{\rm ix}$	1.980 (8)
Mo6—O27	1.882 (6)	Sb10—O36	2.025 (7)
Mo6—O28	1.893 (7)	Sb10—O25$^{\rm ii}$	2.166 (7)
Mo6—O7$^{\rm iii}$	2.231 (7)	Sb10—O47$^{\rm vii}$	2.353 (7)
Mo6—O1$^{\rm iv}$	2.244 (7)	Sb11—O39	1.992 (7)
Mo7—O23$^{\rm v}$	1.760 (6)	Sb11—O42	2.036 (7)
Mo7—O17$^{\rm vi}$	1.761 (7)	Sb11—O27	2.130 (6)
Mo7—O29	1.843 (7)	Sb11—O46$^{\rm vii}$	2.347 (7)
Mo7—O30	1.864 (7)	Sb12—O40$^{\rm ix}$	2.016 (7)
Mo7—O20	2.162 (7)	Sb12—O28$^{\rm iii}$	2.050 (7)
Mo7—O14	2.243 (7)	Sb12—O43	2.060 (7)
Mo8—O24$^{\rm vii}$	1.739 (8)	Sb12—O45$^{\rm vii}$	2.490 (7)
Mo8—O18$^{\rm viii}$	1.743 (8)	Sb12—O4$^{\rm iii}$	2.494 (7)
Mo8—O31	1.849 (8)	Sb13—O38$^{\rm v}$	1.980 (7)
Mo8—O32	1.862 (7)	Sb13—O45	1.997 (7)
Mo8—O13	2.224 (7)	Sb13—O29	2.149 (7)
Mo8—O19	2.243 (7)	Sb13—O43$^{\rm vii}$	2.318 (7)
Sb1—O33	1.993 (8)	Sb14—O35$^{\rm v}$	1.946 (7)
Sb1—O34	2.004 (8)	Sb14—O46	2.035 (7)
Sb1—O3	2.136 (7)	Sb14—O30$^{\rm v}$	2.051 (7)
Sb1—O35	2.394 (8)	Sb14—O39$^{\rm vii}$	2.483 (7)
Sb1—O26	2.680 (8)	Sb14—O16$^{\rm ix}$	2.503 (7)
Sb2—O36	1.968 (7)	Sb15—O44$^{\rm vii}$	2.014 (6)
Sb2—O37	2.042 (7)	Sb15—O47	2.034 (7)
Sb2—O10	2.051 (6)	Sb15—O31	2.058 (7)
Sb2—O38	2.547 (7)	Sb15—O36$^{\rm vii}$	2.484 (7)
Sb2—O25$^{\rm ii}$	2.572 (8)	Sb15—O22$^{\rm vii}$	2.528 (7)
Sb3—O39	1.989 (7)	Sb16—O41$^{\rm vii}$	1.940 (6)
Sb3—O40	2.011 (7)	Sb16—O48	1.989 (7)
Sb3—O4$^{\rm iv}$	2.036 (7)	Sb16—O32$^{\rm vii}$	2.140 (6)
Sb3—O27	2.560 (6)	Sb16—O34$^{\rm vii}$	2.340 (8)

Symmetry codes: (i) $-x, -y, -z$; (ii) $1 - x, -y, -z$; (iii) $1 - x, 1 - y, -z$; (iv) $-x, 1 - y, -z$; (v) $1 - x, -y, 1 - z$; (vi) $-x, -y, 1 - z$; (vii) $1 - x, 1 - y, 1 - z$; (viii) $-x, 1 - y, 1 - z$; (ix) $1 + x, y, z$.

The intensities of the measured reflections have been corrected for Lorentz and polarization factors. The Mo and Sb atoms were introduced by analogy with the Sb_2WO_6 structure (Castro *et al.*, 1994) and refined isotropically (*SHELXL*96; Sheldrick, 1996). The 48 independent O atoms were located from difference Fourier summation. Calculations were performed with anisotropic displacement parameters for Mo and Sb atoms, and isotropic displacement parameters for O atoms. For clarity in the figures, the displacement ellipsoids were plotted at arbitrary probability levels.

Data collection: *CAD*-4 *EXPRESS* (Enraf–Nonius, 1993). Cell refinement: *CAD*-4 *EXPRESS*. Data reduction: *CADAK* (Savariault, 1991). Program(s) used to solve structure: *SHELXS*96 (Sheldrick, 1990). Program(s) used to refine structure: *SHELXL*96 (Sheldrick, 1996). Molecular graphics: *ORTEP*II (Johnson, 1976). Software used to prepare material for publication: *SHELXL*96.

AC thanks the CEMES/CNRS (France) for their kind welcome and the DGES (Spain) for financial support.

Supplementary data for this paper are available from the IUCr electronic archives (Reference: JZ1184). Services for accessing these data are described at the back of the journal.

References

Buttrey, D. J., Vogt, T., Wildgruber, U. & Robinson, W. R. (1994). *J. Solid State Chem.* **111**, 118–127.

Castro, A., Millan, P. & Enjalbert, R. (1995). *Mater. Res. Bull.* **30**, 871–882.

Castro, A., Millan, P., Enjalbert, R., Snoeck, E. & Galy, J. (1994). *Mater. Res. Bull.* **29**, 871–879.

Castro, A., Millan, P., Martinez-Lope, M. J. & Torrance, J. B. (1993). *Solid State Ionics*, **63–65**, 897–901.

Elzen, A. F. van den & Rieck, G. D. (1973). *Acta Cryst.* B**29**, 2436–2438.

Enraf–Nonius (1994). *CAD*-4 *EXPRESS*. Version 5.1/1.2. Enraf–Nonius, Delft, The Netherlands.

Galy, J., Meunier, G., Andersson, S. A. & Åström, A. (1975). *J. Solid State Chem.* **13**, 142–159.

Johnson, C. K. (1976). *ORTEP*II. Report ORNL-5138. Oak Ridge National Laboratory, Tennessee, USA.

Laarif, A., Theobald, F. R., Vivier, H. & Hewat, A. W. (1984). *Z. Kristallogr.* **167**, 117–124.

Ling, C. L., Withers, R. L., Rae, A. D., Schmid, S. & Thompson, J. G. (1996). *Acta Cryst.* B**52**, 610–615.

Millan, P., Ramirez, A. & Castro, A. (1995). *J. Mater. Sci. Lett.* **14**, 1657–1660.

North, A. C. T., Phillips, D. C. & Mathews, F. S. (1968). *Acta Cryst.* A**24**, 351–359.

Ramirez, A., Enjalbert, R., Rojo, J. M. & Castro, A. (1997). *J. Solid State Chem.* **128**, 30–37.

Savariault, J. M. (1991). *CADAK. Programme de Réductions des Données du CAD*-4. CEMES, Toulouse, France.

Sheldrick, G. M. (1990). *Acta Cryst.* A**46**, 467–473.

Sheldrick, G. M. (1996). *SHELXL*96. *Program for the Refinement of Crystal Structures*. University of Göttingen, Germany.

Acta Cryst. (1997). C**53**, 1529–1531

$Cs_3H(SeO_4)_2$ at 300 K by High-Resolution Neutron Powder Diffraction

RAINER SONNTAG,[a] ROLF MELZER,[b] THOMAS WESSELS[c] AND PABLO G. RADAELLI[d]

[a]Hahn-Meitner-Institut, Glienickerstr. 100, D-14109 Berlin, Germany, [b]Institut für Angewandte Geowissenschaften I, TU Berlin/Sekr. BH1, D-10587 Berlin, Germany, [c]Laboratorium für Kristallographie, ETH-Zentrum, CH-8092 Zürich, Switzerland, and [d]Institute Laue-Langevin, 156X, F-38042 Grenoble, France. E-mail: sonntag@hmi.de

(*Received 29 October 1996; accepted 23 May 1997*)

Abstract

The monoclinic room-temperature structure of tricaesium hydrogen bis[tetraoxoselenate(2−)] was refined from high-resolution neutron powder diffraction data. Special emphasis was given to the precise location of the H atom and the determination of the hydrogen-bond network. A Fourier analysis clearly shows that the H atom is distributed over two symmetry-equivalent positions of half occupancy [H···H = 0.52 (2) Å] around an inversion centre. The hydrogen bridge is non-linear [O—H···O = 173 (2)°] with an O···O distance of 2.506 (7) Å.

Comment

$Cs_3H(SeO_4)_2$ (TCHSe) is a member of a family of compounds with the general formula $M_3H(XO_4)_2$ (M = Rb, Cs, K, NH_4; X = S, Se). The isostructural rhombohedral proton-conducting phases of this family are well known. The two-dimensional proton conductivity results from the disorder of the H atoms over partly occupied symmetry-equivalent positions. Until now, structural studies of this family were mainly performed using X-ray diffraction (for TCHSe see Merinov, Bolotina, Baranov & Shuvalov, 1988, 1991; Merinov, Baranov & Shuvalov, 1990; Ichikawa, Gustafsson & Olovsson, 1992), making it impossible to clarify the exact positions of the light atoms, which is the basic knowledge required for an understanding of the proton-conducting mechanism.

Our group recently performed the first neutron powder diffraction experiments on $Rb_3H(SeO_4)_2$ at different temperatures (Bohn *et al.*, 1995; Melzer, Sonntag & Knight, 1996; Melzer, Wessels & Reehuis, 1996). The only neutron diffraction study of $Cs_3H(SeO_4)_2$ until now was of a deuterated specimen, $Cs_3D(SeO_4)_2$, at 5 K (Belushkin, Ibberson & Shuvalov, 1993). We have recently reported the first-high resolution neutron powder diffraction experiment on the proton-conducting phase of TCHSe at 473 K (Sonntag, Melzer & Knight, 1997). In this work, we present a structural investigation of the hydrogen-bond network in TCHSe at room temperature, based on a high-resolution neutron powder diffraction experiment performed on the D2B instrument of the ILL at Grenoble.

TCHSe at room temperature is monoclinic with space group *C*2/*m*. The structure is built from Cs atoms coordinated by O atoms belonging to SeO_4 tetrahedra. These tetrahedra are linked into isolated pairs by hydrogen bonds. Cs atoms and SeO_4 tetrahedra form mixed layers parallel to a pseudo-hexagonal plane alternating with layers containing only Cs atoms. For a more detailed description of the structure see Bohn *et al.* (1995) and Melzer, Wessels & Reehuis (1996).

The initial parameters for our refinement were taken from Merinov *et al.* (1988). We started the refinement with the H atom situated on the inversion centre in the middle of the hydrogen bridge and with isotropic displacement parameters for all atoms. As the displacement parameter of the H atom refined to a large value, we then determined anisotropic displacement parameters for the H atom. A much better fit was obtained and the *R* fac-